

Chapter 4B

Influence of Structural Variation on Nuclear Localization of DNA-Binding Polyamide-Fluorophore Conjugates

Abstract

A pivotal step forward in chemical approaches to controlling gene expression is the development of sequence-specific DNA-binding molecules that can enter live cells and traffic to nuclei unaided. DNA-binding polyamides are a class of programmable, sequence-specific small molecules that have been shown to influence a wide variety of protein-DNA interactions. We have synthesized over 100 polyamide-fluorophore conjugates and assayed their nuclear uptake profiles in thirteen mammalian cell lines. The compiled dataset, comprising 1300 entries, establishes a benchmark for the nuclear localization of polyamide-dye conjugates.

Compounds in this series were chosen to provide systematic variation in several structural variables, including dye composition and placement, molecular weight, charge, ordering of the aromatic and aliphatic amino-acid building blocks, and overall shape. Nuclear uptake does not appear to be correlated with polyamide molecular weight or with the number of imidazole residues, although the positions of imidazole residues affect nuclear access properties significantly. Generally negative determinants for nuclear access include the presence of a β -Ala-tail residue and the lack of a cationic alkyl amine moiety, whereas the presence of an acetylated 2,4-diaminobutyric acid-turn is a positive factor for nuclear localization. We discuss implications of this data on the design of polyamide-dye conjugates for use in biological systems.

Introduction

Cell-permeable small molecules that preferentially bind to predetermined DNA sequences inside living cells would be useful tools in molecular biology, and perhaps human medicine. Minor groove-binding polyamides containing the aromatic amino acids *N*-methylpyrrole (Py), *N*-methylimidazole (Im), *N*-methyl-3-hydroxypyrrole (Hp), and other related aromatic heterocycles bind DNA with affinities and specificities comparable to naturally occurring DNA-binding proteins.¹⁻⁴ DNA recognition by polyamides is described by a code of side-by-side amino acid pairings that are oriented N→C with respect to the 5'→3'-direction of the DNA helix in the minor groove: Im/Py is specific for G•C, Hp/Py is specific for T•A, and Py/Py binds both A•T and T•A.¹

Polyamides have been shown to influence a wide variety of protein-DNA interactions in solution,⁵⁻¹⁵ yet similar experiments in cell culture have proven to be dependent on cell-type.¹⁶⁻¹⁸ Studies with fluorescent Bodipy-labeled polyamides indicate that these conjugates are excluded from the nuclei of most cells, with the notable exceptions of lymphoid and myeloid cell types.^{19,20} One report suggested that the fluorophore itself may play a role in cellular uptake: an eight-ring polyamide-fluorescein conjugate was shown to accumulate in the nuclei of HCT-116 colon cancer cells.²¹ Expanding upon this lead, we recently described a set of polyamide-fluorescein conjugates that localized to the nuclei of thirteen live mammalian cell lines.²² Relatively small structural alterations, such as differences in Py/Im sequence, caused dramatic changes in nuclear localization. The current study seeks to elucidate more fully the structural requirements for nuclear localization of polyamide-fluorophore conjugates. This is a minimum first step in exploring the use of these DNA-binding ligands for gene

modulation in cell culture experiments.

Results

We have synthesized 100 polyamide-fluorophore conjugates, whose chemical structures are shown along with schematic ball-and-stick representations (e.g., Figure 4.6). We examined the nuclear localization properties of these compounds in thirteen mammalian cell lines, representing eleven human cancers, one human transformed kidney cell line, and one murine leukemia cell line. Cells were allowed to incubate with polyamide-fluorophore conjugate in the surrounding medium (2 or 5 μ M, as indicated, 10-14 h) and the extent of nuclear uptake was analyzed by confocal microscopy. Polyamide-dye conjugates display a range of uptake efficiencies, varying from strong nuclear concentration, producing brightly stained nuclei with little or no signal in the medium or cytoplasm, to an absence of nuclear accumulation, in which case the molecules may be trapped in vesicles or excluded from cells entirely. Within a single sample, staining is usually remarkably homogenous, displaying minimal cell-to-cell variation.

The extent of nuclear localization for each sample was assigned one of four qualitative ratings, and these data are organized into tables showing the ball-and-stick structure of each compound and the level of uptake in each cell line (e.g. Figure 4.7). A thin vertical line separates data collected in adherent cell lines (*left*, MCF-7 through 293) from data collected in suspended cell lines (*right*, Jurkat through NB4). Within these two sets, more permissive cell lines – those that generally display stronger nuclear staining with polyamide conjugates – are towards the left. Thus, MCF-7 and Jurkat are the most

permissive cell types of the adherent and suspended cells, respectively. Shaded groupings of compounds indicate structurally related conjugates, as discussed in the text.

Dye composition

We synthesized conjugates **1-20** to investigate the effect of the fluorophore moiety on nuclear localization (Figure 4.6). Figure 4.7 shows the uptake profiles of these compounds. Polyamides **1-6** are conjugated to fluorescein derivatives, and all show strong nuclear staining in the cell lines tested. There appears to be flexibility in the specific type of chemical linkage, as thiourea (**1**, resulting from FITC conjugation) and amide (**2-6**) linkers are effective, including the extended thioether amide-linkage of Oregon Green[®] (OG) 514 in compound **5**. Fluorination of the aromatic rings is well tolerated (**3-5**), and replacing the carboxylic acid with a sulfonic acid (as in OG 500 conjugate **4**) appears to be somewhat beneficial in several cell lines (compare compounds **3** and **4**). The greater photostability of the fluorinated OG derivatives, as compared to fluorescein, may be advantageous for fluorescence imaging applications.^{28,29} The JOE fluorophore, a fluorescein derivative with chloro and methoxy substituents, has red-shifted absorption and emission spectra compared to fluorescein, such that their spectra can be distinguished. JOE conjugate **6** shows moderate to strong uptake in all cell lines, providing a second color for multicolor fluorescence applications.

Compounds **7-11**, conjugated to rhodamine derivatives, display poorer nuclear localization profiles than analogous fluorescein conjugates. The sulfonated rhodamine-dye Alexa 488 is a highly photostable alternative to fluorescein; however, conjugate **7** was completely excluded from the nuclei of all cells tested. Rhodamine green derivative

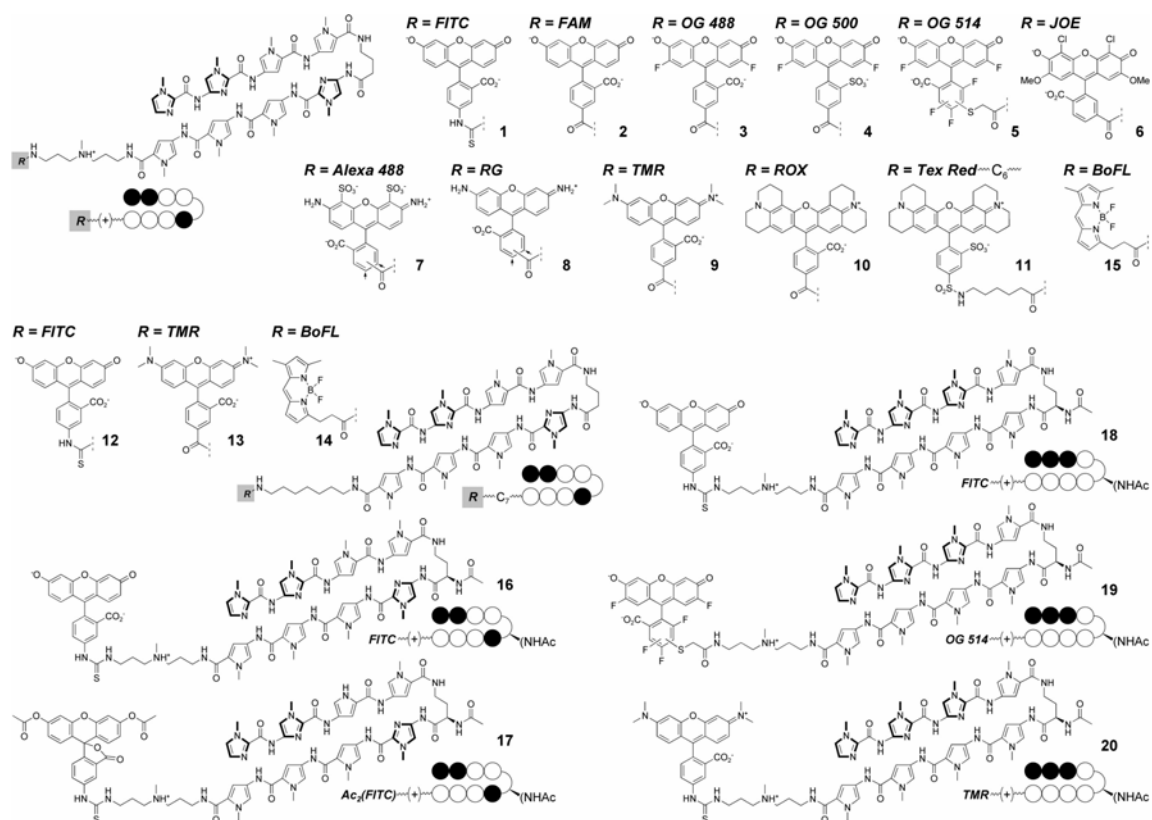


Figure 4.6 Dye composition. Chemical and ball-and-stick structures of compounds 1-20, testing the effect of differing dye composition on cellular uptake.

8, lacking sulfonates, showed slightly stronger nuclear localization, particularly in adherent cell lines. The additional alkyl groups in tetramethyl rhodamine (TMR) conjugate **9** impart enhanced uptake properties in most cell lines, compared to **8**. Depending upon the cell type (as well as the ring sequence and composition of the polyamide, *vide infra*), polyamide-TMR conjugates may be useful because of the photostable, red/orange fluorescence of the TMR dye. Compound **10** is conjugated to the related ROX fluorophore, and conjugate **11** incorporates a Texas Red fluorophore with a hexanoic acid spacer, a dye/linker combination that has been used to label polyamides for telomere staining experiments.³⁰ Both polyamides, **10** and **11**, are consistently excluded


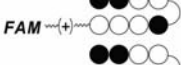
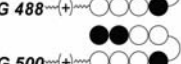


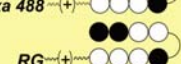



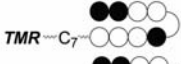
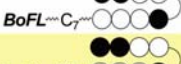
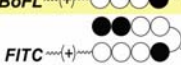


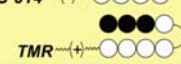
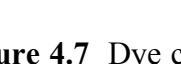
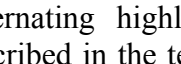
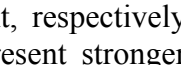
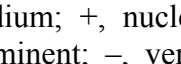
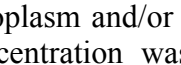
		MCF-7	HeLa	PC3	LN-CaP	SK-BR-3	DLD-1	786-O	293	Jurkat	CEM	MEG-01	MEL	NB4
	1 ^a	++	++	++	++	++	+	++	++	++	++	++	++	++
	2	++	++	++	++	++	++	++	++	++	++	++	++	++
	3 ^b	+	++	+	++	+	++	++	++	++	++	+	+	+
	4	++	++	++	++	++	++	++	++	++	++	++	++	++
	5	++	++	++	++	++	++	++	++	++	++	++	++	++
	6 ^b	++	++	++	+	+	+	++	++	++	++	+	+	+
	7 ^b	--	--	--	--	--	--	--	--	--	--	--	--	--
	8	+	+	+	+	--	+	--	--	--	--	--	--	--
	9 ^b	++	+	+	+	++	--	--	--	++	+	+	+	--
	10	--	--	--	--	--	--	--	--	--	--	--	--	--
	11	--	--	--	--	--	--	--	--	--	--	--	--	--
	12 ^a	+	--	--	--	+	--	--	--	--	--	--	--	--
	13 ^b	--	--	--	--	--	--	--	--	--	--	--	--	--
	14 ^b	--	--	--	--	--	--	--	--	--	--	--	--	--
	15 ^a	--	--	--	--	--	--	--	--	--	--	--	--	--
	16 ^a	++	++	++	++	++	++	++	++	++	++	++	++	++
	17 ^b	++	++	++	++	++	++	++	+	++	++	++	++	++
	18	+	++	++	+	++	+	+	+	+	++	+	--	--
	19	++	++	++	++	++	++	+	++	++	++	++	--	--
	20	--	--	--	--	--	--	--	--	--	--	--	--	--

Figure 4.7 Dye composition: uptake profile of polyamides **1-20** in thirteen cell lines. Alternating highlighting indicates groups of chemically similar polyamides, as described in the text. Data for adherent and suspended cells are towards the left and right, respectively, separated by a light gray vertical line. Lighter shades of blue represent stronger nuclear localization. ++, Nuclear staining exceeds that of the medium; +, nuclear staining less than or equal to that of the medium, but still prominent; –, very little nuclear staining, with the most fluorescence seen in the cytoplasm and/or medium; --, no nuclear staining. Except where noted, polyamide concentration was 2 μM . ^aPolyamide described previously,²² assayed at 5 μM . ^bAssayed at 5 μM .

from live cells.

In compounds **12-14**, a seven-carbon alkyl chain links the dye—FITC, TMR, and Bodipy FL (BoFL), respectively—to the polyamide. For comparison, BoFL derivative **15**, incorporating the standard cationic triamine linker, is also included. As described previously, the BoFL conjugate in this motif displays only minimal evidence of nuclear access in live cells.²² For each alkyl-linked conjugate, the loss of the tertiary amine in the linker worsened the uptake profile (compare **1** and **12**, **9** and **13**, and **15** and **14**). It was shown previously that alkyl-linked conjugate **12** performed much more poorly than triamine-linked conjugate **1**, and that addition of an amino group at the turn residue, using the chiral $\text{H}_2\text{N}\gamma$ -turn, restored most of the uptake properties (see compound **78**, below).²² In contrast, adding amino groups to the dye, as in alkyl-linked TMR conjugate **13**, abolishes nuclear access.

Acetylating fluorescein produces a non-fluorescent, uncharged moiety; cleavage of the acetates by esterases subsequently unmask the fluorophore. Polyamide **16**, as described previously,²² demonstrates that the $\text{AcHN}\gamma$ -turn does not impede uptake, and the analogous diacetyl-FITC conjugate **17** stains nuclei with similar effectiveness. It should be noted that no special effort was taken to remove esterases from the growth medium, such that some amount of **16** is likely to be in solution when cells are treated with **17**. Polyamides **18-20** have the same number of Im and Py residues as compounds **1-17** but in a different sequence. With the exception of the less permissive suspended cells MEL and NB4, FITC conjugate **18** (an isomer of **16**) and OG 514 conjugate **19** display modest to strong nuclear staining. In contrast, TMR conjugate **20** is a very poor nuclear stain. Comparing analogous compounds, conjugates **18** and **19** display only slightly poorer

uptake profiles than those of conjugates **1** and **5**, respectively, whereas TMR conjugate **20** is a much worse nuclear stain than polyamide **9**. Such comparisons indicate that modifications such as ring sequence and fluorophore structure interact to affect nuclear uptake in ways that are not yet predictable.

Second-Generation Rings

We have recently described several second-generation aromatic ring systems that improve the DNA-binding properties of polyamides.^{3,4} When paired against Py, a chlorothiophene (Ct) residue at the N-terminal cap position targets a T•A base pair.⁴ The hydroxybenzimidazole (Hz) moiety, incorporated as part of a dimeric subunit, appears to be a chemically stable replacement for the Hp residue,³ and a CtHz-cap dimer has recently been found to target the sequence 5'-TT-3' (R.M. Doss, M.A. Marques, S. Foister, and P.B. Dervan, unpublished results). Figure 4.8 shows the chemical structures of polyamide-fluorophore conjugates incorporating second-generation rings, and Figure 4.9 displays their uptake properties.

Ct-cap compounds **21-24** have the same ring sequence but different dyes. Polyamides **21-23**, conjugated to fluorescein derivatives, display strong nuclear localization, whereas TMR conjugate **24** displays a moderate uptake profile that is generally similar to **9** and better than **20**. Conjugates **25-28** demonstrate the effects of different ring sequences on nuclear uptake of thiophene-cap conjugates. Whereas **25** displays good to excellent nuclear staining, its isomer **26** is excluded from all cells tested. Other conjugates with three contiguous Im residues – methylthiophene-cap polyamide **27**, and ten-ring hairpin **28** – also display very poor uptake properties. The only

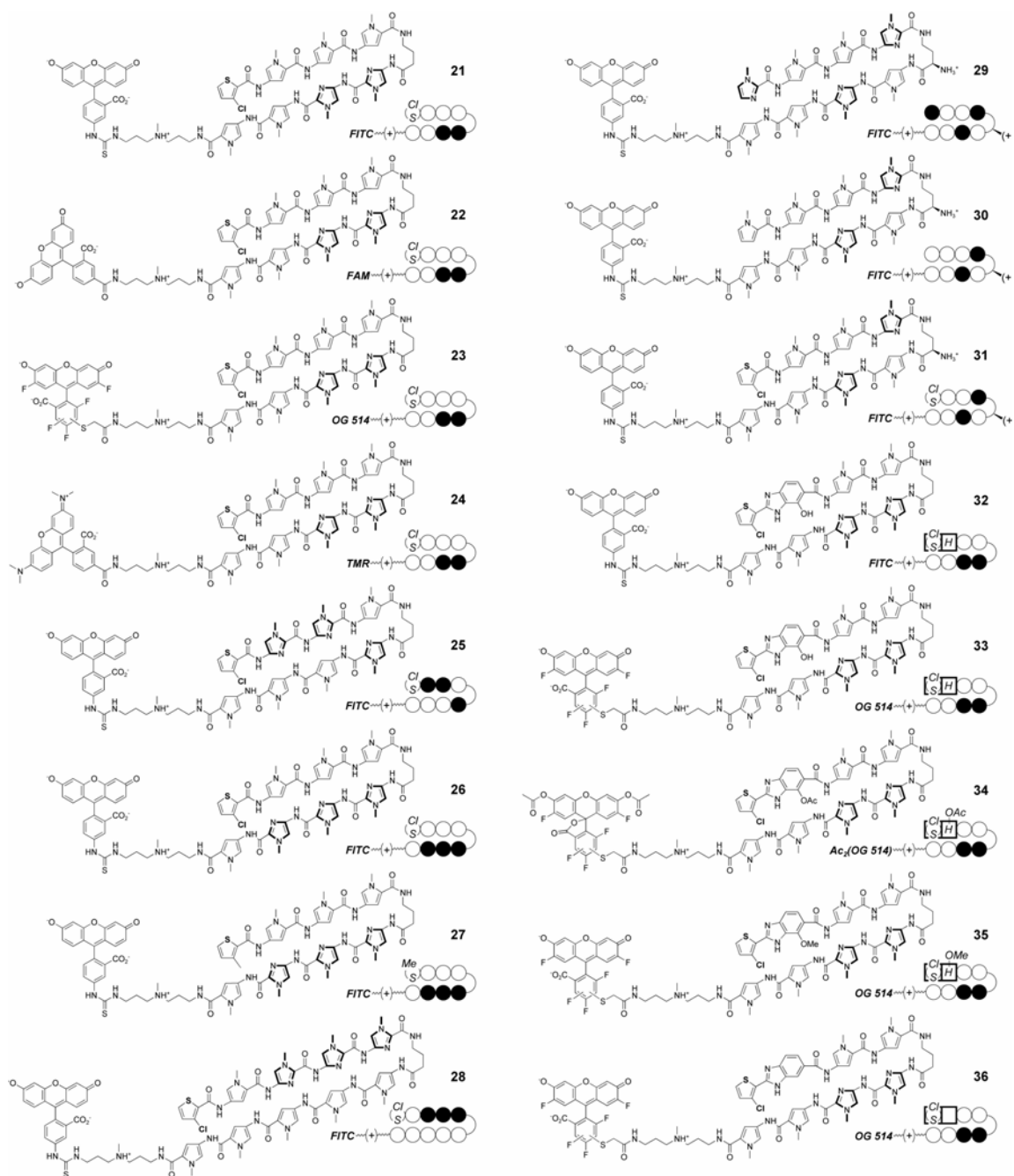


Figure 4.8 Second-generation rings. Chemical and ball-and-stick structures of compounds 21-36, testing the effect of new aromatic rings on cellular uptake.

structure. Compounds **29** and **31**, with Im and Ct caps, respectively, are excellent nuclear stains, whereas Py-cap polyamide **30** is significantly less effective. It is remarkable that an Im→Py conversion (**29** to **30**), formally an N→C-H shift, reduces nuclear uptake, but the more dramatic Im→Ct conversion affects uptake very little.

Based on the ring sequence of **21-24**, compounds **32-36** incorporate variants of the benzimidazole ring system. Although polyamides incorporating the Hz unit display favorable DNA-binding properties, FITC conjugate **32** stains the nuclei of only a few cell lines, and OG 514 conjugate **33** stains only MCF-7 and LNCaP cells. Modifications to the hydroxyl group, including acetylation (**34**) and conversion to a methoxy group (**35**), did not improve the uptake profile. Complete removal of the hydroxyl group (**36**) allows nuclear localization in many cell lines, though the uptake profile does not correlate with the general permissiveness of the cell types. Furthermore, removing the hydroxyl eliminates the ability to distinguish between A•T and T•A base pairs at that position.³

Extended Hairpin Motif

Figure 4.10 shows the chemical structures of polyamide-dye conjugates **37-46** with C-terminal unpaired rings, and Figure 4.11 shows their uptake profiles. The molecules are grouped into pairs that differ with respect to the conjugated dye. Although the DNA-binding properties of the extended hairpin motif have not been studied as extensively as those of fully ring-paired hairpin polyamides,^{31,32} extended hairpin polyamides have been shown to interfere with NF-κB—DNA interactions¹³ and to label specific heterochromatic regions of human chromosomes.²⁹ Furthermore, tandem polyamides with extended hairpin subunits have been used to stain telomeres³⁰ and to

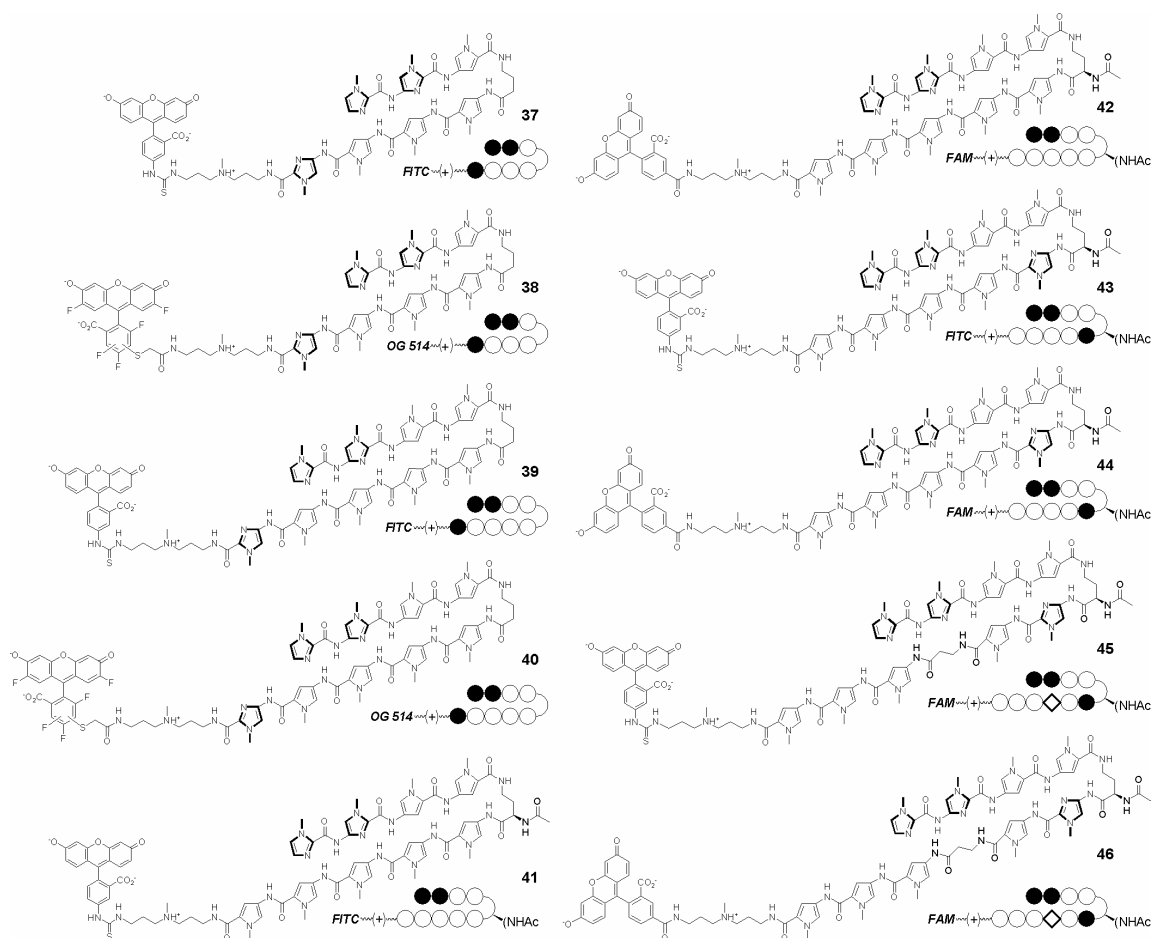


Figure 4.10 Extended hairpins. Chemical and ball-and-stick structures of compounds **37-46**, testing the effect of extensions to the hairpin motif on cellular uptake.

displace a viral transcription factor from DNA.³³ Overall, conjugates **37-46** display good to excellent nuclear localization properties.

Seven-ring polyamides **37** and **38**, conjugated to FITC and OG 514, respectively, are moderately effective nuclear stains. The larger nine-ring FITC conjugate **39** displays a significantly improved uptake profile, whereas OG 514 conjugate **40** is similar to the seven-ring hairpins. Polyamides **41** and **42** have a similar nine-ring core, but with a single unpaired Py residue and a chiral ^{AcHN} γ -turn. Both the FITC and FAM conjugate (**41** and **42**, respectively) are excellent nuclear stains. From these compounds, one

	MCF-7	HeLa	PC3	LN-CaP	SK-BR-3	DLD-1	786-O	293	Jurkat	CEM	MEG-01	MEL	NB4
37 FITC	++	+	+	+	++	+	-	-	++	++	-	--	--
38 OG 514	+	++	+	+	+	+	+	+	+	+	--	--	-
39 FITC	++	++	++	++	+	+	++	+	++	++	-	+	+
40 OG 514	+	+	+	-	+	+	+	+	++	+	--	-	+
41 FITC (NHAc)	++	++	++	+	++	++	++	+	++	++	++	+	++
42 FAM (NHAc)	++	++	++	++	++	++	++	++	++	++	++	++	++
43 FITC (NHAc)	+	++	++	+	+	+	+	+	++	+	++	-	--
44 FAM (NHAc)	++	++	++	++	++	+	+	--	++	+	++	++	+
45 FITC (NHAc)	+	+	+	+	+	--	--	+	+	--	-	-	+
46 FAM (NHAc)	++	++	++	+	--	+	+	+	++	++	++	++	++

Figure 4.11 Extended hairpins: uptake profile of polyamides **37-46**. Symbols are defined in Figure 4.7.

Py→Im substitution gives **43** and **44**, respectively. In this case, FAM conjugate **44** performs better than FITC conjugate **43**. Based on a motif that was used in studies with NF- κ B,¹³ compounds **45** and **46** have two unpaired Py residues. Again, the FAM conjugate displays the better uptake profile, strongly staining the nuclei of eight of the thirteen cell lines.

Larger Polyamides

Somewhat larger than the extended hairpin polyamides **37-46** are fully ring-paired hairpins **47-54** and **56-62**. Figure 4.12 shows the structures of dye conjugates **47-62**, and Figure 4.13 displays their uptake profiles. Many of these compounds incorporate the flexible β -Ala residue, which is often substituted for Py to allow polyamides to adapt to sequence-dependent DNA microstructure and flexibility.^{34,35} In general, conjugates of

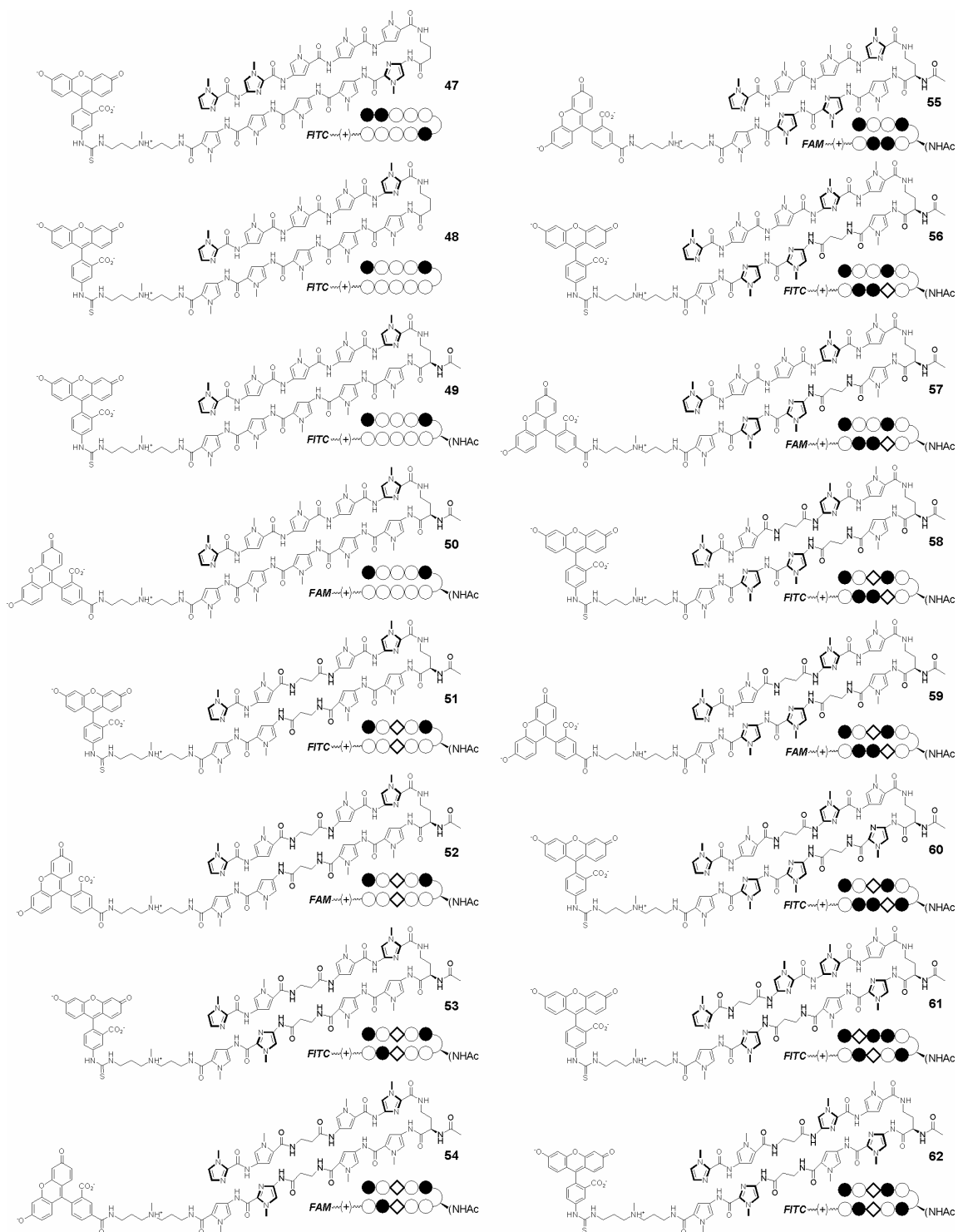


Figure 4.12 Larger polyamides. Chemical and ball-and-stick structures of compounds 47-62, testing the effect of molecular size on cellular uptake.

		MCF-7	HeLa	PC3	LN-CaP	SK-BR-3	DLD-1	786-O	293	Jurkat	CEM	MEG-01	MEL	NB4
	47 ^a	--	-	--	-	-	-	--	--	--	--	--	--	--
	48	+	+	+	--	--	+	-	+	+	+	-	-	-
	49	+	++	++	++	+	+	+	+	+	+	+	+	--
	50	+	++	++	+	++	+	+	-	+	-	+	+	-
	51	+	+	+	+	-	+	+	-	+	--	+	+	+
	52	+	-	+	+	--	--	--	--	-	--	--	+	-
	53	+	++	+	+	+	-	--	--	--	--	--	-	+
	54	+	--	-	-	+	--	--	+	-	++	--	-	+
	55	--	--	--	--	--	-	-	--	--	--	--	--	--
	56	+	-	+	--	--	-	--	--	--	--	--	--	--
	57	+	+	+	+	--	-	--	--	+	-	-	--	--
	58	+	+	+	+	-	-	+	-	--	-	--	-	--
	59	+	+	+	+	-	+	+	-	+	+	-	+	+
	60	-	+	--	+	-	-	-	--	--	--	--	--	-
	61	-	--	--	--	--	--	--	--	--	--	--	--	--
	62	-	-	--	-	-	-	--	-	--	--	--	--	--

Figure 4.13 Larger polyamides: uptake profile of polyamides 47-62. Symbols are defined in Figure 4.7. Except where noted, polyamide concentration was 2 μM . ^aPolyamide described previously,²² assayed at 5 μM .

this motif display poor to moderate nuclear staining, although there are scattered exceptional cases.

Conjugate 47, described previously, displayed a particularly poor uptake profile. From 47, an Im \rightarrow Py substitution produces 48, which displays some nuclear staining in eight cell lines. Chiral ^{AcHN} γ -turn analogs of 48, conjugates 49 and 50, display improved uptake properties, accessing the nuclei of most of the cell types, and showing excellent staining in some of the more permissive adherent cells. Polyamides 51 and 52 (related to

49 and **50**, respectively, by Py→ β -Ala substitutions of the central residues), are less efficient nuclear stains, with FAM conjugate **52** performing significantly more poorly. Compounds **53** and **54** result from an additional Py→Im substitution. FITC conjugate **53** accesses the nuclei of the more permissive adherent cells, whereas FAM conjugate **54** displays a scattered uptake profile.

Polyamides **55-59** are designed to target essentially the same 6-bp DNA sequence. Eight-ring hairpin **55**, included as a reference, is excluded from all cell nuclei, whereas the larger polyamides access nuclei somewhat more successfully. In this set, internal β -Ala substitution and FAM-conjugation are both positive determinants for nuclear uptake; accordingly, conjugate **59** is the most effective nuclear stain. Polyamide **60** is related to **58** by a Py→Im substitution, and **60** displays a much poorer uptake profile. Inverting the strands of **60** produces **61** – the result of a formal 180° rotation of the ring core – which is excluded from the nuclei of all cells tested. Conjugate **62** is based on a motif that has been employed in a variety of studies;^{18,20,36} however this FITC conjugate is excluded from cell nuclei.

C-terminal β -Ala Residues

In a previous study, we noted that adding β -Ala residue to the C-terminal (“tail”) position of a polyamide-dye conjugate could have dramatic effects on nuclear localization.²² We therefore synthesized the molecules shown in Figure 4.14 to investigate the effects of β -Ala-tail residues. To allow for the possibility that the added β -Ala would enhance uptake, precursor ring systems were chosen to have a range of uptake efficiencies (Figure 4.15). The polyamides are grouped by their core ring

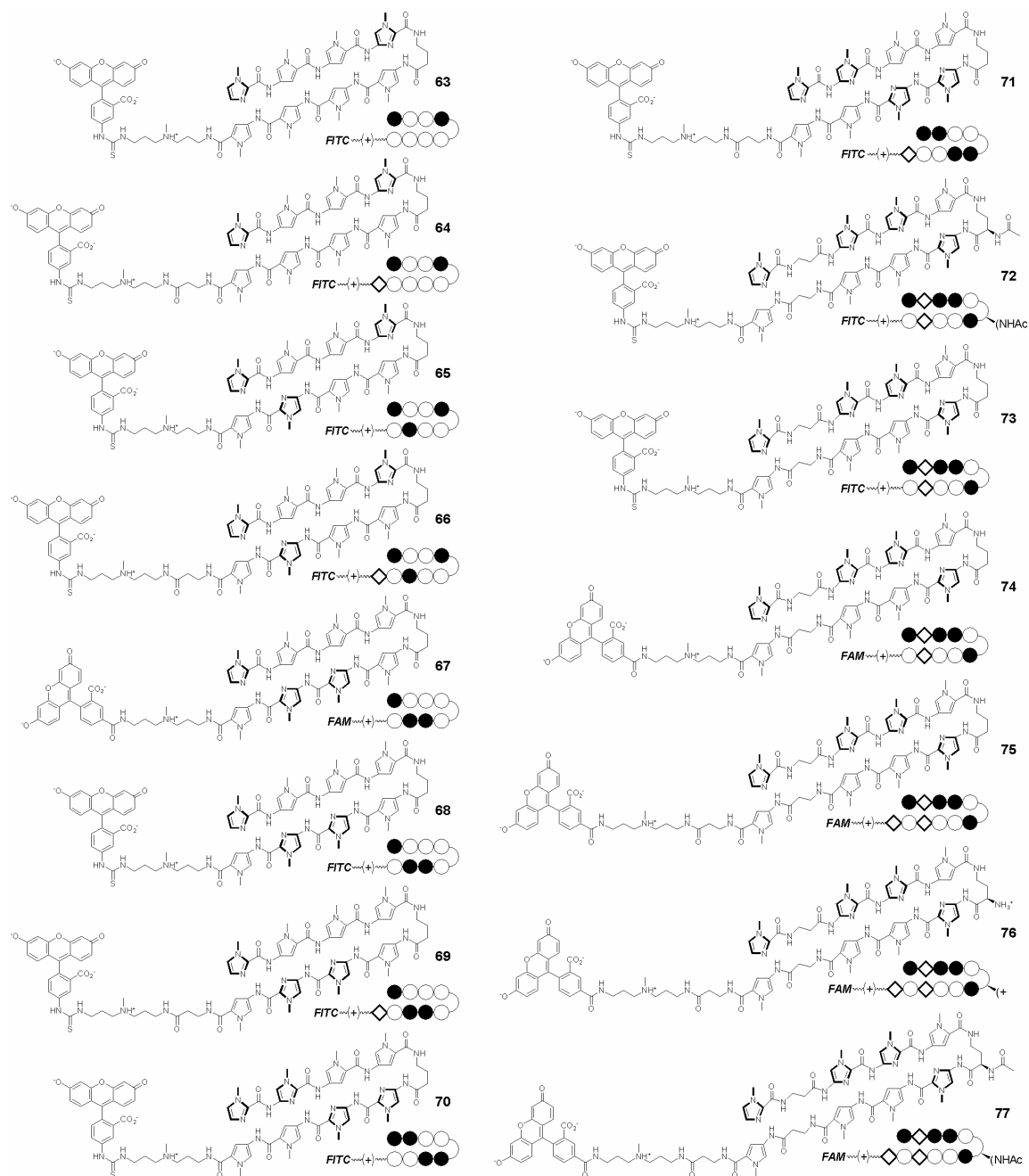


Figure 4.14 β -Alanine tails. Chemical and ball-and-stick structures of compounds 63-77, testing the effect of molecular size on cellular uptake.

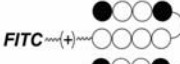







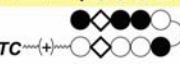





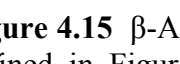
	MCF-7	HeLa	PC3	LN-CaP	SK-BR-3	DLD-1	786-O	293	Jurkat	CEM	MEG-01	MEL	NB4
 63^a	++	++	++	++	++	++	++	++	++	++	++	++	++
 64	++	++	++	++	+	++	+	++	++	++	++	++	++
 65^a	+	++	+	+	+	+	+	+	++	++	+	--	-
 66	+	-	--	--	--	-	--	-	--	--	--	--	--
 67^b	+	-	-	-	--	+	--	--	-	-	--	--	--
 68	+	+	+	--	--	+	--	+	-	-	--	--	--
 69	--	-	-	--	--	-	--	--	--	--	--	--	--
 70^a	+	+	-	-	-	-	--	-	--	-	--	--	--
 71	+	--	-	--	-	+	--	-	--	-	--	-	--
 72	++	++	++	++	++	++	++	+	++	++	+	--	--
 73	+	-	--	--	-	--	-	--	--	--	-	--	--
 74	--	--	--	--	-	--	--	-	--	--	--	--	--
 75	--	--	--	--	--	--	--	--	--	--	--	--	--
 76	-	--	--	--	-	--	-	--	--	--	--	--	--
 77	--	+	--	--	+	-	--	--	-	-	--	+	--

Figure 4.15 β -Alanine tail residues: uptake profile of polyamides **63-77**. Symbols are defined in Figure 4.7. Except where noted, polyamide concentration was 2 μ M. ^aPolyamide described previously,²² assayed at 5 μ M. ^bAssayed at 5 μ M.

sequence. In almost every case, adding a β -Ala-tail residue reduces nuclear uptake efficiency. Indeed, even in cases in which both samples have the same qualitative rating, the conjugate with a β -Ala-tail shows slightly less intense nuclear staining.

Conjugate **63** is an excellent nuclear stain, and addition of a β -Ala-tail residue (compound **64**) affects uptake only minimally. In contrast, polyamide **65** displays a moderate to good uptake profile, and its β -Ala-tail analog **66** shows very poor nuclear staining. Although FITC conjugate **68** (an isomer of polyamide **1**) accesses nuclei slightly more effectively than FAM conjugate **67**, it is nonetheless a rather weak stain,

and addition of a β -Ala-tail residue (conjugate **69**) completely inhibits nuclear access. Conjugate **70**, described previously,²² accesses the nuclei of only two cell lines, and addition of a β -Ala-tail residue (compound **71**) does not change the uptake profile significantly. Polyamides **72-77** have the same ring sequence, but vary with respect to dye structure, turn substitution, and the presence of a β -Ala-tail residue. Of this series, only FITC conjugate **72** (with an ^{AcHN} γ -turn and lacking a β -Ala-tail) displays an excellent uptake profile. Polyamide **72** is isomeric with compounds **58** and **62**, and of these three conjugates, **72** displays by far the most efficient nuclear staining. Interestingly, although the overall uptake profile of FAM conjugate **77** is relatively poor, this β -Ala-tail polyamide is one of three compounds in Figure 4.15 that can access the nuclei of MEL cells.

Turn-linked conjugates

To investigate other dye-attachment points, conjugates were synthesized linked to the chiral turn element (**80-88**, Figure 4.16). For comparison, this set includes tail-conjugated polyamides **78**, **79**, and **89**. Figure 4.17 presents the uptake profiles of **78-89**. Polyamides **78** and **79** are conjugated to FITC through seven- and six-methylene spacers, respectively. Neither compound stains nuclei as effectively as the analogous conjugate **1**, although **79** is quite close. Compared to **78**, polyamide **80** exchanges the positions of the cationic amine group and the dye linker. These turn-linked FITC conjugates are excellent nuclear stains, and the presence of an additional amine (in **81**) or a β -Ala-tail residue (in **82**) does not impede nuclear uptake. The sole exception is compound **81** in NB4, a cell line which was previously observed to exclude polyamide-dye conjugates with added

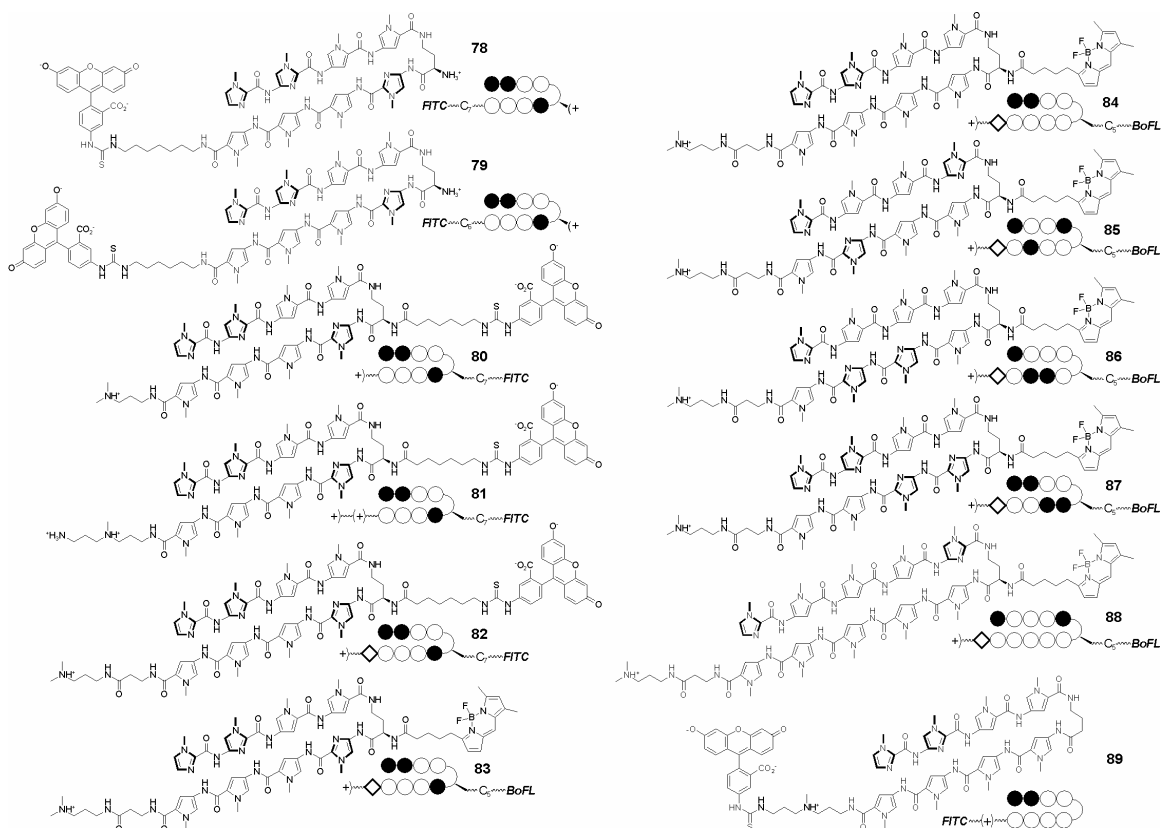


Figure 4.16 $\text{H}_2\text{N}\gamma$ -turn-linked conjugates. Chemical and ball-and-stick structures for polyamides **78-89**, testing the effect of removing the dye moiety to the $\text{H}_2\text{N}\gamma$ -turn.

positive charges.²²

Hairpin polyamides **83-88**, linked to BoFL through the turn, differ with respect to Py/Im composition, and are analogous to the tail-linked FITC conjugates **1**, **89**, **65**, **68**, **70**, and **48**, respectively. Although each eight-ring BoFL turn-conjugate is a less effective stain than the corresponding FITC tail-conjugate, relative uptake efficiency within each motif appears to be influenced primarily by ring composition. Indeed, ranked by average effectiveness, **83** \approx **84** > **85** > **86** \approx **87**, and correspondingly, **1** \approx **89** > **65** > **68** \approx **70**. Ten-ring BoFL-turn conjugate performs similarly to its FITC-tail analog **48**, although the $\text{AcHN}\gamma$ -turn derivative **49** is a significantly better nuclear stain than either


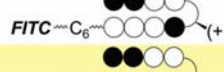
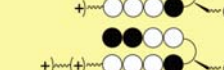

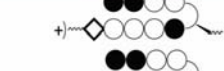




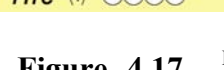
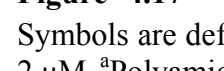
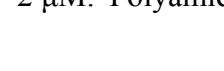
	MCF-7	HeLa	PC3	LN-CaP	SK-BR-3	DLD-1	786-O	293	Jurkat	CEM	MEG-01	MEL	NB4
 78 ^a	+	++	+	++	+	+	+	+	+	++	+	+	+
 79	++	++	++	++	++	++	+	++	++	++	++	++	++
 80 ^b	++	++	++	++	++	++	++	++	++	++	++	+	+
 81 ^b	++	++	++	++	++	++	++	++	++	++	++	++	--
 82 ^b	++	++	++	++	++	++	++	++	++	++	++	+	+
 83	+	++	++	++	+	--	--	--	+	+	--	--	+
 84	+	++	++	++	+	--	--	--	+	+	--	--	+
 85	--	+	+	++	--	--	--	--	+	+	--	--	--
 86	--	--	--	--	--	--	--	--	--	--	--	--	--
 87	--	--	--	--	--	--	--	--	+	--	--	--	--
 88	+	+	++	++	--	--	--	--	+	+	--	--	--
 89 ^a	++	++	++	++	++	++	++	++	++	++	++	++	++

Figure 4.17 $H_2N\gamma$ -Turn-linked conjugates: uptake profile of polyamides **78-89**. Symbols are defined in Figure 4.7. Except where noted, polyamide concentration was 2 μ M. ^aPolyamide described previously,²² assayed at 5 μ M. ^bAssayed at 5 μ M.

conjugate. The favorable uptake properties of some of these BoFL-turn conjugates—particularly in more permissive cell lines—is somewhat surprising in comparison to the poor nuclear localization profile of tail-linked BoFL conjugate **15** (Figure 4.7).

Shapes

Beyond hairpin polyamides derivatized at the turn, a variety of unique polyamide shapes have been described, including *N*-methyl substituted hairpins,^{13-15,37,38} cycles,^{39,40} U-pins,²⁶ H-pins,^{27,41} and tandem hairpins.^{30,33,42} Figure 4.18 shows the chemical structures of dye conjugates of various shapes, and Figure 4.19 presents their uptake profiles.

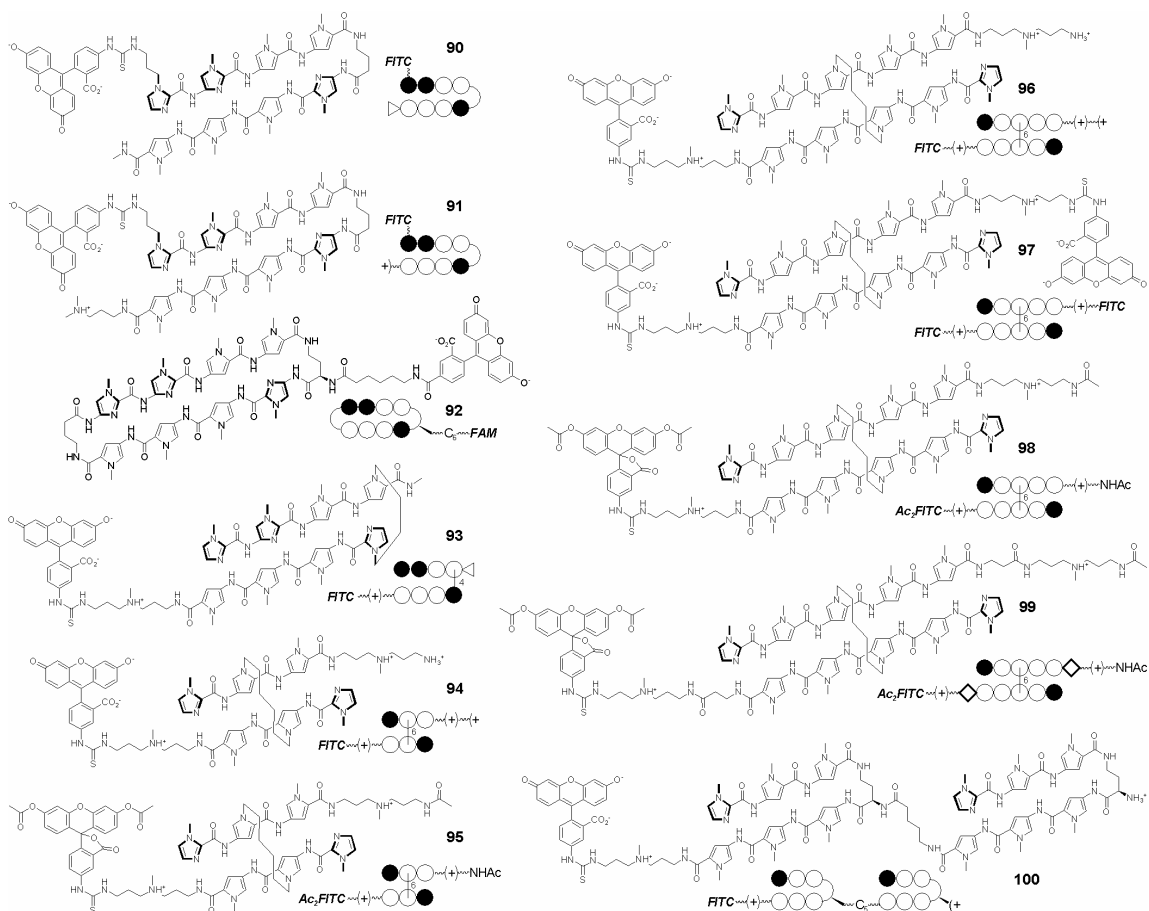


Figure 4.18 Shape variation. Chemical and ball-and-stick structures of compounds **90-100**, testing the effect of molecular shape on cellular uptake.

FITC conjugate **90**, linked through an *N*-propylamine Im-cap residue, is a poor nuclear stain, as described previously.²² After evaluating other compounds, and noting that effective compounds incorporated a cationic amine group, we synthesized compound **91** (an isomer of conjugate **1**), which demonstrated good to excellent uptake properties. Correspondingly, cyclic polyamide **92** displayed a very poor uptake profile. In contrast, U-pin polyamide **93** is a moderately good nuclear stain, especially in adherent cells.

Uptake data for H-pin polyamides indicates that a motif cannot be evaluated by a handful of molecules alone. Of the six-ring H-pins, **95** (the peracetylated derivative of

	MCF-7	HeLa	PC3	LN-CaP	SK-BR-3	DLD-1	786-O	293	Jurkat	CEM	MEG-01	MEL	NB4
90 ^a	+	--	--	--	-	+	--	--	--	+	-	--	--
91	++	++	++	++	++	+	++	+	++	+	++	--	++
92	-	--	--	--	--	--	--	--	--	--	--	--	--
93 ^b	+	+	+	++	++	+	+	+	+	-	-	--	+
94	--	--	--	--	--	--	--	--	--	--	--	--	--
95	-	--	--	--	--	--	--	--	--	- ^c	+ ^c	- ^c	- ^c
96 ^b	--	--	--	--	--	--	--	--	--	--	--	--	--
97 ^b	--	--	--	--	--	--	--	--	--	--	--	--	--
98	+ ^c	+	+	+	+ ^c	+	+	-	++	++	++	-	--
99	- ^c	- ^c	- ^c	- ^c	- ^c	- ^c	-	- ^c	+ ^c	+ ^c	- ^c	--	- ^c
100 ^b	--	--	--	--	--	--	--	--	--	--	--	--	--

Figure 4.19 Shape variations: uptake profile of polyamides **90-100**. Symbols are defined in Figure 4.7. Except where noted, polyamide concentration was 2 μM . ^aPolyamide described previously,²² assayed at 5 μM . ^bAssayed at 5 μM . ^cHighly heterogeneous uptake profile. Some cells display clear nuclear localization, while others show none. The value shown is an approximate average.

94) showed highly heterogeneous staining in a small number of cell lines. Within a single microscope frame, some cells were brightly stained, while others were completely dark – where indicated, the data in Figure 4.17 represent a rough average across the cells. Ten-ring H-pins **96** and **97** were excluded from all cells tested, whereas **98** (the ten-ring analog of **95**) showed good to excellent staining in all but the least permissive cell lines. In line with trends observed earlier, adding C-terminal β -Ala residues (compound **99**) diminishes the uptake efficiency.

Tandem hairpins can target longer sequences of DNA than standard hairpin polyamides, so the complete exclusion of FITC conjugate **100** from cells is somewhat disappointing. However, it is possible that another tandem, containing a different Py/Im sequence, dye, or other variation might access the nuclei of some cell types.

Short Peptides

The successful staining of the nuclei of mammalian cells with polyamides labeled with fluorescein and other similar dyes permits many transcription inhibition experiments to be attempted with confidence that a negative result is not due to exclusion of active compound from genomic DNA. However, there are many applications requiring polyamides to be conjugated to peptide and small molecule moieties. The uptake characteristics of these compounds must be good in order to proceed with *in vivo* experiments. As a first-pass attempt, a small set of polyamide-peptide-fluorophore conjugates have been prepared (Figure 4.20) and their uptake characteristics measured. The synthetic scheme for **101-105** is shown in Figure 4.21. In general, the uptake of these conjugates is poor, with the compounds being excluded from or sequestered in the cytoplasm of all cell lines studied (Figure 4.22). Further work will be necessary to determine whether this is a general characteristic of polyamide-peptide conjugates, or if some privileged structures might permit good nuclear uptake.

Discussion

From this sea of data, certain trends can be discerned. There does not appear to be any clear correlation between molecular weight and nuclear uptake. Indeed, additional residues can improve uptake (compare, e.g., **37** and **39**, or **55** and **59**), or impede it (compare **1** and **47**, or **48** and **63**). Similarly, a Py \rightarrow β -Ala exchange, which reduces molecular weight, may intensify or diminish nuclear staining (Figure 4.15). The acetylated ^{AcHN} γ -turn, which adds molecular weight compared to an unsubstituted γ -turn, is one of the few consistently positive factors for nuclear localization (for example,

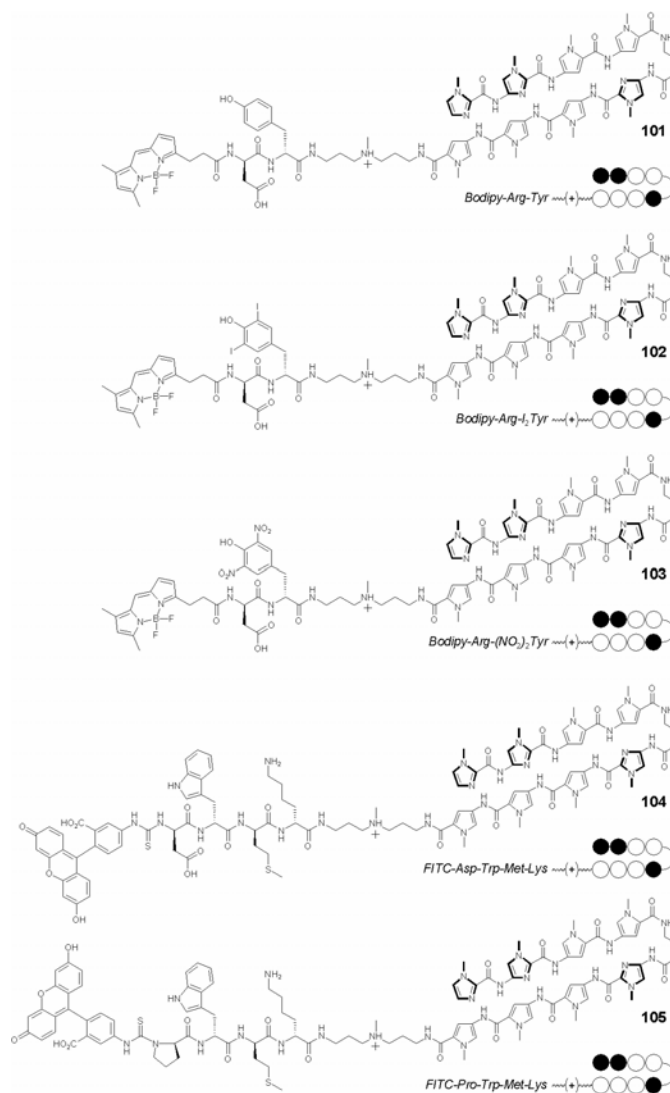


Figure 4.20 Small peptides. Chemical and ball-and-stick structures of compounds **101-105**, testing the effect on cellular uptake of the addition of small peptide moieties to polyamide-fluorophore conjugates.

compare **1** and **16**, **48** and **49**, or **72** and **73**). Generally negative determinants for nuclear access include the presence of a β -Ala-tail residue and the lack of a cationic alkyl amine moiety.

Although there is no general correlation between the number of Im residues and uptake efficiency, the positions of Im residues clearly affect nuclear access. For example,

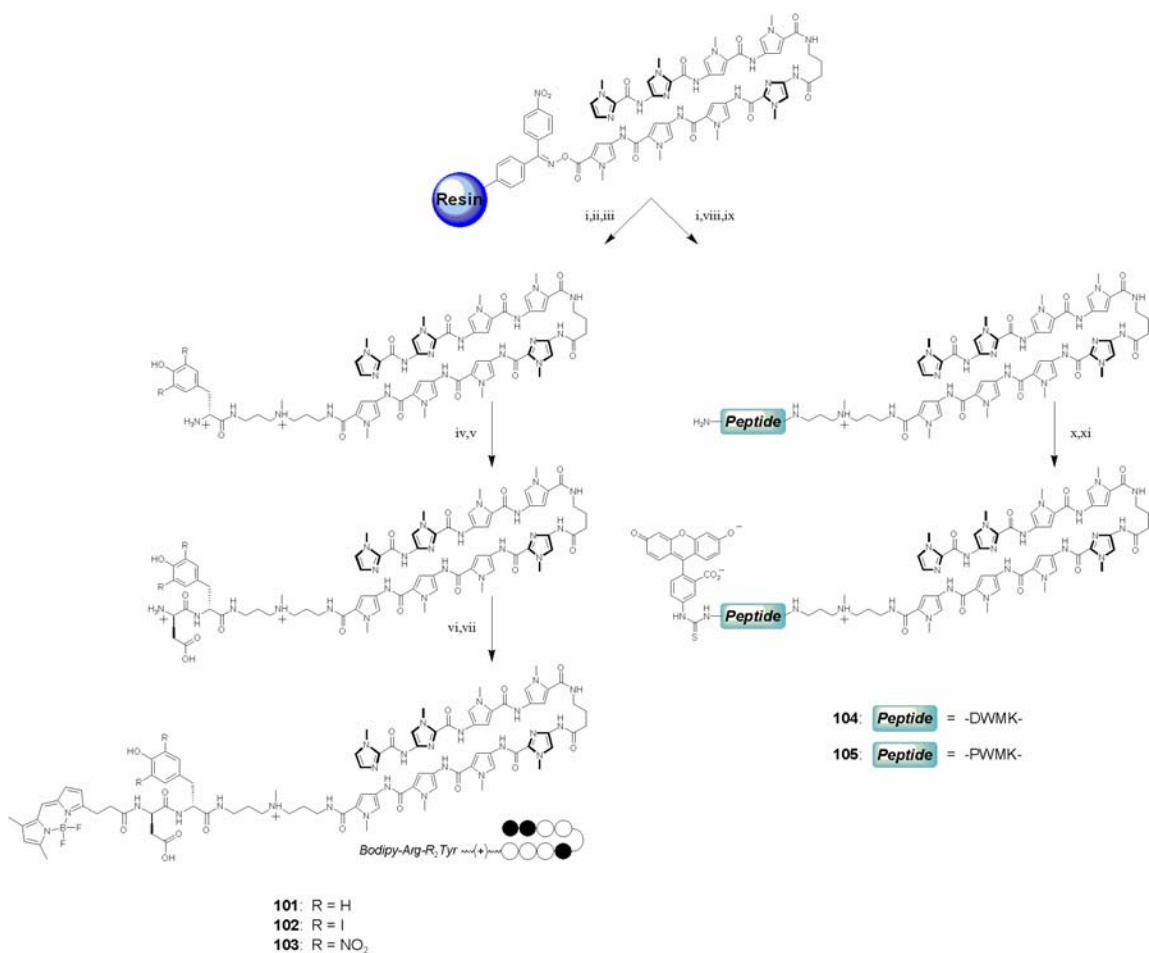


Figure 4.21 Synthesis of small peptide conjugates. (i) 3,3'-diamino-*N*-methyl-dipropylamine, 6 hrs at 37°C. (ii) R₂Tyr, DCC, HOBt, DIEA, DMF. (iii) 20% (v/v) piperidine/DMF. (iv) (*D*) Asp-Ph₂ipr, DCC, HOBt, DIEA, DMF. (v) 20% (v/v) piperidine/DMF. (vi) Bodipy-FL, DCC, HOBt, DIEA, DMF. (vii) 20% (v/v) TFA/CH₂Cl₂. (viii) Peptide, DCC, HOBt, DIEA, DMF. (ix) 20% (v/v) piperidine/DMF. (x) FITC, DIEA, DMF. (xi) 20% (v/v) TFA/CH₂Cl₂.

structural isomers often display very different uptake profiles (compare eight-ring polyamides **1**, **65**, and **68**, or larger conjugates **58**, **62**, and **72**). Furthermore, a Py→Im exchange is nearly always a negative determinant for nuclear access (except at the cap position, compare **29** and **30**), and the impact is highly dependent on the position of the residue and the overall polyamide motif. For example, in eight-ring polyamide-dye conjugates the effect of a single Py→Im exchange may be very small (**89** versus **1**),

modest (**63** versus **65**), or severe (**1** versus **70**).

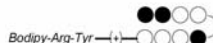
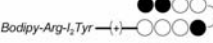
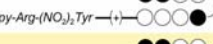
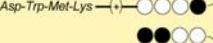
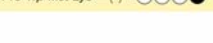
		MCF	HeLa	PC3	LN-CaP	DLD-1	786-O	Jurkat	CEM	MEG-01	MEL	NB4
	101	--	--	--	--	-	--	--	+	--	--	--
	102	--	--	--	--	--	--	--	--	--	--	--
	103	--	--	--	--	--	--	--	+	--	--	--
	104	-	-	--	--	--	--	--	--	--	--	--
	105	--	--	--	--	--	--	--	--	--	--	--

Figure 4.22 Small peptides: uptake profile of polyamides **101-105**. Symbols are defined in Figure 4.7. Polyamide concentration was 2 μ M.

The role of charge in nuclear uptake is particularly intriguing, though uptake does not appear to correlate with net charge. At neutral pH, fluorescein conjugates that efficiently access cell nuclei have a net charge of -1 (the majority of conjugates, exemplified by **1**) or a net charge of 0 (such as **29**, **31**, and **81**). However, polyamide-fluorescein conjugates have been observed to accumulate in acidic vesicles (reference 21 and data not shown), in which the pH is between \sim 4.5 and 6.⁴³ Because the pK_a 's of the phenolic protons of fluorescein and OG derivatives are \sim 6.4 and \sim 4.7, respectively,⁴⁴ the phenol moiety will be fully or partially protonated in acidic vesicles. Thus, in such subcellular structures, polyamide-fluorescein conjugates such as **1** would have a net charge of 0, whereas conjugates such as **29** would have a net charge of +1.

It may be that the ability to change protonation state enhances the nuclear localization properties of fluorescein conjugates relative to rhodamine and bodipy derivatives, which are pH insensitive. TMR and BoFL conjugates having a net charge of 0 (compounds **13** and **14**) or +1 (compounds **8-11**, **15** and **83-88**) all perform significantly more poorly than analogous fluorescein conjugates. It is remarkable that moving the

positive charge from the linker to the dye is not tolerated whatsoever (compare triamine-linked FAM conjugate **2** and alkyl-linked TMR conjugate **13**, Figure 4.7), whereas relatively well-tolerated alterations include moving the positive charge to the turn (compare FITC conjugates **1** and **78**) and moving the dye to the cap residue, effectively increasing the distance between the anionic and cationic moieties (compare FITC conjugates **1** and **91**).

Conjugation to fluorescein appears to facilitate uptake for this class of molecules, though it is not essential: TMR conjugate **9** is an excellent nuclear stain in several cell lines, and turn-linked BoFL conjugates **83**, **84**, and **88** display improved uptake profiles compared to the tail-linked BoFL derivative **15**. Indeed, polyamides without any attached fluorophore have been shown to induce biological effects in living cells, albeit in a limited number of cell types. Whereas **62** was excluded from cells, an analog of **62** without a dye-label altered gene expression in live lymphoid cells, and a non-dye-labeled chorambucil derivative of **62** was shown to alkylate genomic DNA in live cells.²⁰ This example highlights the distinct properties of dye-conjugated versus unlabeled polyamides. One cannot be considered as a “proxy” for the other, regarding cellular localization characteristics or other properties. Fluorescent polyamide conjugates are unique because their ability to access nuclei can be assessed directly, and it is our intent to use such labeled polyamides in biological studies involving live cell systems.

Although the uptake data presented here do not allow for prediction of nuclear uptake properties *a priori*, rough design guidelines are apparent. Synthesizing and analyzing a small, focused library of polyamide-fluorophore conjugates appears to be the optimal approach. Key points of variation are ring sequence (if possible on a given

target), dye composition (FITC, FAM, OG 514, etc.) and position of conjugation, turn substitution (γ -turn or $^{AcHN}\gamma$ -turn), and β -Ala incorporation. Examples of such focused libraries are compounds **55-59**, **72-77**, and **96-99**.

For use in live-cell studies, polyamides must now be optimized along three axes: DNA-binding affinity and specificity, *in vitro* biochemical activity, and nuclear localization. For the first and second axes, assays such as DNase footprinting, gel shift, and *in vitro* transcription are well established, and studies based on these techniques continue to expand the scope and utility of DNA-binding polyamides.^{3,12,15,45} The current study employs an assay based on confocal microscopy to establish a benchmark dataset, comprising 1300 entries, for nuclear localization of DNA-binding polyamide-dye conjugates. Live-cell studies with these compounds are currently in progress, as are efforts to elucidate the energy-dependent mechanism of uptake.²² Understanding nuclear accessibility in a wide variety of living cells is a minimum first step toward chemical regulation of gene expression with this class of molecules.

Experimental

Chemicals

Polyamides were synthesized by solid phase methods on Boc- β -ala-PAM resin (Peptides International, Louisville, KY)²³ or on Kaiser oxime resin (Nova Biochem, Laufelfingen, Switzerland).²⁴ Synthetic protocols for second-generation building blocks (incorporated into polyamides shown in Figure 4.8 and polyamides **90** and **91**, Figure 4.17) are essentially as described.^{2-4,25} The polyamide precursor to compound **92** was synthesized as follows:

Cbz- γ -ImImPyPy- (R)^{FmocHN} γ -ImPyPyPy-Oxime was prepared using the Kaiser oxime resin as previously described.²⁴ The Fmoc-protecting group was cleaved by 20% (v/v) piperidine/DMF cleavage (4 x 3 min) and replaced by a *t*-Boc group upon treatment with Boc₂O, DIEA, and DMF. The polyamide was cleaved from resin by first swelling dried resin in dioxane (500 mg resin, ~1 mL dioxane) for 1 hr, and then adding a solution of 3:1 dioxane:NaOH (1M aqueous) and allowing the resin to cleave at 37°C for 36 hrs. Filtration of the resin and a second treatment with fresh cleavage solution yields further crude product, all of which was purified by C₁₈ reverse-phase HPLC and lyophilized to provide polyamide as a white powder (~10% yield).

Cbz- γ -ImImPyPy- (R)^{BocHN} γ -ImPyPyPy-COOH (8 μ mol) was dissolved in 1:1 absolute EtOH:CH₂Cl₂ (5 mL), to which was added first Pd(OAc)₂ (0.2 g, 950 μ mol), then ammonium formate (0.3 g, 4.7 mmol). The solution was stirred at room temperature under Ar for 20 min. The solution was centrifuged to remove precipitated PdO, purified by C₁₈ reverse-phase HPLC, and lyophilized to provide polyamide as a white powder (~25% yield).

H₂N- γ -ImImPyPy- (R)^{BocHN} γ -ImPyPyPy-COOH (2.2 μ mol) was dissolved in DMF (4 mL). K₂CO₃ (0.11 g, 0.8 mmol) that had been dried at 130°C was added and the mixture was stirred for 1 hr. DPPA (14.5 μ L, 67 μ mol) was added and the mixture was stirred for 4 hrs. The solution was concentrated to a brown film, which was treated with 80% (v/v) TFA/CH₂Cl₂ for 45 min, concentrated, purified by C₁₈ reverse-phase HPLC, and lyophilized to provide polyamide as a white powder (~25% yield). Polyamide cyclo-(γ -ImImPyPy- (R)^{H₂N} γ -ImPyPyPy-) was treated with fluorescein amide-C₆ linker

succinimidyl ester as with other dye additions, purified, and lyophilized to provide **92** as an orange powder (~50% yield).

U-pin **93** and H-pins **94-99** were synthesized according to methods described in references (26) and (27), respectively. After cleavage with the appropriate amine and reverse-phase HPLC purification, polyamides were dissolved in DMF and treated with diisopropylethylamine (DIEA) (20 eq) followed by the fluorophore in the form of an isothiocyanate, an *N*-hydroxysuccinimidyl ester, or a free acid activated *in situ* with HBTU. Fluorophores were delivered as solutions in DMF or DMSO. After reacting at rt for ~3 h, the resulting dye conjugates were purified by HPLC.

Peracetylated polyamides **17**, **34**, **95**, **98**, and **99** were obtained by treating the precursor polyamides with acetic anhydride and DIEA in DMF for ~30 min. For compounds with a free (*R*)-2,4-diaminobutyric acid ($^{\text{H}_2\text{N}}\gamma\text{-turn}$) moiety (**29-31**, **76**, **78**, **79**, and **100**), the protected $^{\text{FmocHN}}\gamma\text{-turn}$ amine was deprotected (20% piperidine-DMF) and reprotected as the Boc derivative (Boc₂O, DIEA, DMF) immediately prior to cleavage of the polyamide from resin. After conjugation of the dye moiety, these compounds were treated with TFA and purified by HPLC.

Compounds **101-105** were prepared as shown in Figure 4.21. The peptides for **104** and **105** were prepared on SASRIN resin (Bachem), cleaved with 1% (v/v) TFA in CH₂Cl₂, and purified on silica, retaining the side-chain protection on the aspartic acid and tryptophan residues. The identity and purity of each compound was verified by analytical HPLC, UV-visible spectroscopy, and matrix-assisted laser desorption ionization/time-of-flight mass spectrometry (MALDI-TOF). Table 4.2 lists the masses calculated and found for all conjugates. All fluorescent dye reagents were from Molecular Probes. Chemicals

not otherwise specified were from Sigma-Aldrich.

Cell Cultures

The human cancer cell lines MCF-7, PC3, LNCaP, DLD-1, 786-O, Jurkat, CCRF-CEM (CEM), MEG-01, and NB4 were cultured in a 5% CO₂ atmosphere at 37°C in supplemented RPMI medium 1640. The human cancer cell line HeLa, the murine leukemia cell line MEL, and the transformed human kidney cell line 293 were grown as above in supplemented DMEM. The human cancer cell line SK-BR-3 was cultured as above in supplemented McCoy's medium. All media were supplemented with 10% fetal bovine serum (Irvine Scientific) and 1% penicillin/streptomycin solution (Sigma).

Confocal Microscopy

Adherent cell lines (MCF-7, HeLa, PC3, LNCaP, SK-BR-3, DLD-1, 786-O, and 293) were trypsinized for 5–10 min at 37°C, centrifuged for 5 min at 5°C at 900 g, and resuspended in fresh medium to a concentration of 1.25×10^6 cells per ml. Suspended cell lines (Jurkat, CEM, MEG-01, MEL, and NB4) were diluted in fresh medium to the same concentration. Incubations were performed by adding 150 µl of cells into culture dishes equipped with glass bottoms for direct imaging (MatTek, Ashland, MA). Adherent cells were grown in the glass-bottom culture dishes for 24 h. The medium was then removed and replaced with 147 µl (or 142.5 µl) of fresh medium. Then 3 µl (or 7.5 µl) of the 100 µM polyamide solution was added for final polyamide concentration of 2 µM (or 5 µM), as noted in the data tables. Cells were incubated in a 5% CO₂ atmosphere at 37°C for 10–14 h. Suspended cell line samples were prepared in a similar fashion, omitting

trypsinization. These samples were then incubated as above for 10–14 h. Imaging was performed with a x40 oil-immersion objective lens on a Zeiss LSM 5 Pascal inverted laser scanning microscope. The optical slice was set to 2.2 μm . Images were line-averaged 2, 4, 8, or 16 times and were obtained at a 0.8 $\mu\text{s}/\text{pixel}$ scanning rate. Polyamide-dye conjugate fluorescence and visible light images were obtained using standard filter sets appropriate for fluorescein, rhodamine, or Texas Red.

Acknowledgements

We are grateful to the National Institutes of Health for support (Grant GM57148) and for predoctoral support to T.P.B. and R.M.D. (Grant T32-GM08501), to the Howard Hughes Medical Institute for a fellowship to B.S.E., and to the National Science Foundation for a predoctoral fellowship to S.F. Mass spectral analyses were performed in the Mass Spectrometry Laboratory of the Division of Chemistry and Chemical Engineering of Caltech, supported in part by National Science Foundation Materials Research Science and Engineering program.

Table 4.2 Mass spectrometry data for compounds 1-105.

Compound	M+(ion)	calc'd	found	Compound	M+(ion)	calc'd	found
1	H	1584.6	1584.5	51	H -FITC	1393.7	1393.9
2	H	1553.6	1553.4	52	H	1751.7	1751.9
3	H	1589.6	1589.5	53	H -FITC	1394.7	1395.0
4	H	1625.6	1625.6	54	H	1752.7	1752.9
5	H	1689.6	1689.5	55	H	1611.6	1611.7
6	Na	1703.6	1703.6	56	H -FITC	1446.7	1447.0
7	H	1711.6	1711.7	57	H	1804.7	1804.8
8	H	1551.7	1551.8	58	H -FITC	1395.7	1396.0
9	H	1607.7	1607.7	59	H	1753.7	1753.5
10	H	1711.8	1711.8	60	H -FITC	1396.7	1396.7
11	H	1896.8	1896.8	61	H -FITC	1396.7	1396.6
12	H	1569.6	1569.6	62	H -FITC	1395.7	1395.6
13	H	1592.7	1592.5	63	H -FITC	1194.6	1194.6
14	-F	1434.7	1434.1	64	H	1654.7	1654.8
15	Na	1490.7	1490.7	65	H	1584.6	1585.1
16	H	1641.6	1641.5	66	H	1655.7	1655.9
17	H -Ac ₂ FITC	1274.6	1274.6	67	H	1553.1	1553.1
18	H	1641.6	1640.7	68	H -FITC	1195.6	1195.7
19	H	1746.6	1746.6	69	H -FITC	1266.6	1266.7
20	H	1664.7	1664.7	70	H	1585.6	1585.2
21	H -FITC	1231.5	1231.6	71	H	1656.7	1656.8
22	H	1589.5	1589.6	72	Na -FITC	1417.7	1417.7
23	H	1725.5	1725.6	73	H	1727.7	1727.7
24	H	1643.6	1643.8	74	H	1696.7	1696.7
25	H -FITC	1232.5	1232.6	75	H	1767.7	1767.7
26	H -FITC	1232.5	1232.3	76	H	1782.7	1782.6
27	H -FITC	1212.5	1212.5	77	H	1824.8	1824.5
28	H -FITC	1476.6	1476.0	78	H	1584.6	1584.7
29	H	1599.6	1599.6	79	Na	1592.6	1592.4
30	H	1598.7	1598.6	80	H	1683.7	1683.7
31	H	1635.5	1636.1	81	H	1726.7	1726.7
32	H -FITC	1241.5	1241.6	82	H	1754.7	1754.6
33	H	1735.5	1735.4	83	Na	1562.7	1562.5
34	H -OG514	1283.5	1283.2	84	Na	1561.7	1561.6
35	H	1749.5	1749.6	85	Na	1562.7	1562.6
36	H	1719.5	1719.6	86	Na	1562.7	1562.6
37	H -FITC	1073.5	1073.5	87	Na	1563.7	1563.5
38	H	1567.5	1567.7	88	Na	1805.8	1805.8
39	H -FITC	1317.6	1317.3	89	H	1583.6	1583.6
40	H	1811.6	1812.0	90	H	1513.5	1513.3
41	H -FITC	1373.7	1373.7	91	H	1584.6	1584.6
42	H	1731.7	1731.7	92	H	1636.6	1636.4
43	H -FITC	1374.6	1374.8	93	H	1541.6	1541.6
44	H	1732.7	1732.6	94	H	1438.7	1438.4
45	H -FITC	1445.7	1445.6	95	H	1564.7	1564.3
46	H	1803.7	1804.0	96	H	1926.9	1926.3
47	H -FITC	1461.7	1461.8	97	H	2315.9	2319.0
48	H -FITC	1460.7	1460.7	98	H	2052.9	2052.2
49	H -FITC	1495.7	1495.9	99	H	2195.0	2194.4
50	H	1853.8	1853.9	100	H	2270.9	2271.3

101	H	1747.8	1749.6
102	H	1999.6	1998.7
103	H	1837.8	1838.6
104	H	2144.9	2149.3
105	H	2126.9	2127.6

References

- 1) Dervan, P.B.; Edelson, B.S. *Curr. Opin. Struct. Biol.* **2003**, *13*, 284.
- 2) Briehn, C.A.; Weyermann, P.; Dervan, P.B. *Chem.-Eur. J.* **2003**, *9*, 2110.
- 3) Renneberg, D.; Dervan, P.B. *J. Am. Chem. Soc.* **2003**, *125*, 5707.
- 4) Foister, S.; Marques, M.A.; Doss, R.M.; Dervan, P.B. *Bioorg. Med. Chem.* **2003**, *11*, 4333.
- 5) Dickinson, L.A.; Trauger, J.W.; Baird, E.E.; Ghazal, P.; Dervan, P.B.; Gottesfeld, J.M. *Biochemistry* **1999**, *38*, 10801.
- 6) Dickenson, L.A.; Trauger, J.W.; Baird, E.E.; Dervan, P.B.; Graves, B.J.; Gottesfeld, J.M. *J. Biol. Chem.* **1999**, *274*, 12765.
- 7) McBryant, S.J.; Baird, E.E.; Trauger, J.W.; Dervan, P.B.; Gottesfeld, J.M. *J. Mol. Biol.* **1999**, *286*, 973.
- 8) Chiang, S.Y.; Bürli, R.W.; Benz, C.C.; Gawron, L.; Scott, G.K.; Dervan, P.B.; Beerman, T.A. *J. Biol. Chem.* **2000**, *275*, 24246.
- 9) Wang, C.C.C.; Dervan, P.B. *J. Am. Chem. Soc.* **2001**, *123*, 8657.
- 10) Ehley, J.A.; Melander, C.; Herman, D.; Baird, E.E.; Ferguson, H.A.; Goodrich, J.A.; Dervan, P.B.; Gottesfeld, J.M. *Mol. Cell. Biol.* **2002**, *22*, 1723.
- 11) Yang, F.; Belitsky, J.M.; Villanueva, R.A.; Dervan, P.B.; Roth, M.J. *Biochemistry*, **2003**, *42*, 6249.
- 12) Fechter, E.J.; Dervan, P.B. *J. Am. Chem. Soc.* **2003**, *125*, 8476.
- 13) Wurtz, N.R.; Pomerantz, J.L.; Baltimore, D.; Dervan, P.B. *Biochemistry*, **2002**, *41*, 7604.

- 14) Arora, P.S.; Ansari, A.Z.; Best, T.P.; Ptashne, M.; Dervan, P.B. *J. Am. Chem. Soc.* **2002**, *124*, 13067.
- 15) Arndt, H.-D.; Hauschild, K.E.; Sullivan, D.P.; Lake, K.; Dervan, P.B.; Ansari, A.Z. *J. Am. Chem. Soc.* **2003**, *125*, 13322.
- 16) Gottesfeld, J.M.; Neely, L.; Trauger, J.W.; Baird, E.E.; Dervan, P.B. *Nature*, 1997, *387*, 202.
- 17) Janssen, S.; Cuvier, O.; Muller, M.; Laemmli, U.K. *Mol. Cell.* **2000**, *6*, 1013.
- 18) Wang, Y.D.; Dziegielewski, J.; Wurtz, N.R.; Dziegielewska, B.; Dervan, P.B.; Beerman, T.A. *Nucleic Acids Res.* **2003**, *31*, 1208.
- 19) Belitsky, J.M.; Leslie, S.J.; Arora, P.S.; Beerman, T.A.; Dervan, P.B. *Bioorg. Med. Chem.* **2002**, *10*, 3313.
- 20) Dudouet, B.; Burnett, R.; Dickinson, L.A.; Wood, M.R.; Melander, C.; Belitsky, J.M.; Edelson, B.S.; Wurtz, N.R.; Briehn, C.; Dervan, P.B.; Gottesfeld, J.M. *Chem. Biol.* **2003**, *10*, 859.
- 21) Crowley, K.S.; Phillion, D.P.; Woodard, S.S.; Schweitzer, B.A.; Singh, M.; Shabany, H.; Burnette, B.; Hippenmeyer, P.; Heitmeier, M.; Bashkin, J.K. *Bioorg. Med. Chem. Lett.* **2003**, *13*, 1565.
- 22) Best, T.P.; Edelson, B.S.; Nickols, N.G.; Dervan, P.B. *Proc. Natl. Acad. Sci. U.S.A.* **2003**, *100*, 12063.
- 23) Baird, E.E.; Dervan, P.B. *J. Am. Chem. Soc.* **1996**, *118*, 6141.
- 24) Belitsky, J.M.; Nguyen, D.H.; Wurtz, N.R.; Dervan, P.B. *Bioorg. Med. Chem.* **2002**, *10*, 2767.
- 25) Wurtz, N.R. California Institute of Technology: Pasadena, CA, 2002.

- 26) Heckel, A.; Dervan, P.B. *Chem.-Eur. J.* **2003**, *9*, 3353.
- 27) Olenyuk, B.; Jitianu, C.; Dervan, P.B. *J. Am. Chem. Soc.* **2003**, *125*, 4741.
- 28) Delmotte, C.; Delmas, A. *Bioorg. Med. Chem. Lett.* **1999**, *9*, 2989.
- 29) Gygi, M.P.; Ferguson, M.D.; Mefford, H.C.; Lund, K.P.; O'Day, C.; Zhou, P.; Friedman, C.; van den Engh, G.; Stolowitz, M.L.; Trask, B.J. *Nucleic Acids Res.* **2002**, *30*, 2790.
- 30) Maeshima, K.; Jansses, S.; Laemmli, U.K. *EMBO J.* **2001**, *20*, 3218.
- 31) Trauger, J.W.; Baird, E.E.; Dervan, P.B. *Chem. Biol.* **1996**, *3*, 369.
- 32) Trauger, J.W.; Baird, E.E.; Dervan, P.B. *Angew. Chem.-Int. Ed.* **1998**, *37*, 1421.
- 33) Schaal, T.D.; Mallet, W.G.; McMinn, D.L.; Nguyen, N.V.; Sopko, M.M.; John, S.; Parekh, B.S. *Nucleic Acids Res.* **2003**, *31*, 1282.
- 34) Swalley, S.E.; Baird, E.E.; Dervan, P.B. *Chem.-Eur. J.* **1997**, *3*, 1600.
- 35) Turner, J.M.; Swalley, S.E.; Baird, E.E.; Dervan, P.B. *J. Am. Chem. Soc.* **1998**, *120*, 6219.
- 36) Gottesfeld, J.M.; Belitsky, J.M.; Melander, C.; Dervan, P.B.; Luger, K. *J. Mol. Biol.* **2002**, *321*, 249.
- 37) Rucker, V.C.; Foister, S.; Melander, C.; Dervan, P.B. *J. Am. Chem. Soc.* **2003**, *125*, 1195.
- 38) Bremer, R.E.; Wurtz, N.R.; Szewczyk, J.W.; Dervan, P.B. *Bioorg. Med. Chem.* **2001**, *9*, 2093.
- 39) Herman, D.M.; Turner, J.M.; Baird, E.E.; Dervan, P.B. *J. Am. Chem. Soc.* **1999**, *121*, 1121.

- 40) Baliga, R.; Baird, E.E.; Herman, D.M.; Melander, C.; Dervan, P.B.; Crothers, D.M. *Biochemistry* **2001**, *40*, 3.
- 41) Greenberg, W.A.; Baird, E.E.; Dervan, P.B. *Chem.-Eur. J.* **1998**, *4*, 796.
- 42) Kers, I.; Dervan, P.B. *Bioorg. Med. Chem.* **2002**, *10*, 3339.
- 43) Lodish, H.; Berk, A.; Zipursky, L.S.; Matsudaira, P.; Baltimore, D.; Darnell, J. (2000) *Molecular Cell Biology*. 4th ed. W.H. Freeman and Co., New York, NY.
- 44) Lin, H.J.; Szmecinski, H.; Lakowicz, J.R. *Anal. Biochem.* **1999**, *269*, 162.
- 45) Marques, M.A.; Doss, R.M.; Urbach, A.R.; Dervan, P.B. *Helv. Chim. Acta* **2002**, *85*, 4485.